CHEMISTRY OF MATERIALS

Article

pubs.acs.org/cm

Nanoporous Benzoxazole Networks by Silylated Monomers, Their Exceptional Thermal Stability, and Carbon Dioxide Capture Capacity

Hasmukh A. Patel, Dongah Ko, and Cafer T. Yavuz*

Graduate School of EEWS, Korea Advanced Institute of Science and Technology (KAIST), Daejeon 305-701, Republic of Korea

Supporting Information

ABSTRACT: The pursuit of synthetic routes for design and preparation of nanoporous polymeric networks with inherent permanent microporosity and functionality through bottom-up methodologies remains a driving force in developing CO_2-philic materials. We report nanoporous, processable, benzoxazole-linked covalent organic polymers (Box-COPs) that show exceptional thermal stability up to 576 °C. Box-COPs can be formed into films thanks to the silylation that is used to guide polymeric network formation. Surface areas of up to 606 m^2 g^{-1} and narrow pore sizes of 4.36 Å were observed with a CO_2 uptake capacity of 139.6 mg g^{-1} at 273 K and 1 bar. Box-COPs were stable in boiling water for a week without deteriorating CO_2 capture capacity.

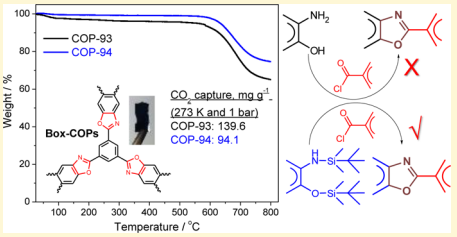

INTRODUCTION

Carbon dioxide (CO_2) emissions from burning fossil fuels exacerbate global warming and contribute greatly to habitat change in the oceans and environment.[1,2] On the basis of the most recent data, low price of fossil fuels, if coupled with untaxed CO_2 emissions, could severely impact our way of living.[3] Measurements of atmospheric CO_2 levels at Mauna Loa, Hawaii, show that the greenhouse gas has accumulated steadily, and spiked above 400 ppm several times in April 2013.[4] A wide spectrum of materials that includes zeolites,[5] mesoporous silica,[6] carbonaceous materials,[7,8] metal−organic frameworks,[9,10] and polymeric membranes[11−15] have been considered for CO_2 capture by absorption, adsorption, and/or separation, yet, none of these materials is competitive enough to replace already established aqueous amine-based CO_2 capture, although the latter is an energy inefficient technology.

Nanoporous amorphous polymers exhibiting permanent microporosity emerge to fulfill promise for applications in gas storage and separation,[16] charge carrier,[17] sensors,[18] and catalysis.[19] Thanks to the wide variety of bond-forming techniques accessible through synthetic organic chemistry, the nanoporous polymeric networks with diverse porosity, thermomechanical stability and functionality have been established.[20−22] The most promising nanoporous polymers are those constructed by rigid monomers through various organic reactions——Yamamoto, Ullmann, Suzuki, Sonogashira−Hagihara couplings, "click" chemistry, and various condensation polymerizations,[23−25] yielding cross-linked polymeric networks with high surface areas, such as COFs, PIMs, HCPs, CMPs, CTFs, TzFs, BILP, POF, COP, CPOP, PCPs, POPs, PPF, SNW, PAFs, PPNs, and several others.[20,26−43] Thermal stability of CO_2 scrubbing materials (e.g., membranes) is desired as exhaust gas mixtures discharge at high temperatures.[11] Polybenzoxazoles are known for their superior thermal stability, and thus their potential in flue gas separations; however, their porous, network polymers are not yet reported. Few examples of linear chains were prepared in polyphosphoric acid (PPA) with excess phosphorus pentoxide as catalyst,[44] which has low solubility in organic solvents and removal of PPA becomes very complicated. This hinders the preparation of benzoxazole network polymers. Fukumaru et al.[45] demonstrated an alternative route for the synthesis of linear benzoxazole polymers by functionalization of the monomers, leading to an improved processability.

In an attempt to produce nanoporous benzoxazole network polymers, hereafter called benzoxazole bridged nanoporous covalent organic polymers (Box-COPs), we coupled trivalent trimesoyl chloride (core) with 4,6-diaminoresorcinol (linker) while screening a wide variety of conditions that include base catalysts, solvents, ratios, temperature and pressure of the reaction. None of the direct pathways has produced the oxazole ring, which needs a ring closure step after amidic adduct is formed. We suspect that the rotational freedom of the linker substituent groups is significantly hindered when network is formed in a random fashion, hence the inability to execute the ring closure. We therefore used silylation, where bulky silyl groups would repel the rest of the linker, which then positions suitable for ring closing (Figure 1a). A subsequent annealing step would unravel the nucleophilic hydroxyls before they attack the amidic carbonyl. In this strategy, the intermediate would also be prone to be soluble in certain solvents. That was exactly what we discovered, in that the silylated prepolymer was soluble in solvents like NMP, leading to a highly sought after property of processability. Briefly, we produced two Box-COPs (COP-93 and COP-94) that were synthesized in three steps: (i) reaction of *tert*-butyldimethylsilyl chloride with 4,6-diaminoresorcinol dihydrochloride and 3,3′-dihydroxybenzi-

Received: August 12, 2014
Published: November 6, 2014

   dx.doi.org/10.1021/cm503627p | Chem. Mater. 2014, 26, 6729−6733

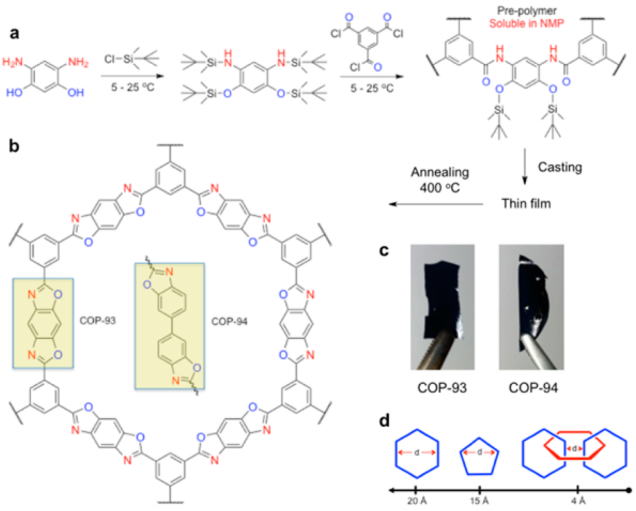

Figure 1. (a) Synthesis of Box-COPs in three steps: (i) silylation of monomers, (ii) prepolymer formation with protected hydroxyl group, and (iii) cyclization at elevated temperature. (b) Hypothetical hexagon macrocyclic unit for COP-93. (c) Annealed thin film strips of Box-COPs: COP-93 and 94. (d) Pore size distribution of COP-93 (4.13 Å) indicates interpenetration of macrocycles, hexagons, and pentagons, or both.

dine in *N,N*-dimethylformamide in the presence of triethylamine results in silylated monomers (protection step); (ii) silylated monomers reacted with 1,3,5-benzenetricarbonyl trichloride in *N*-methyl-2-pyrrolidone (NMP) produce prepolymers COP-93-P and COP-94-P (prepolymer formation step); and (iii) annealing of prepolymers at 400 °C to form Box-COPs (porous polymer formation step).

Although Box-COPs are formed from rigid monomers, the lack of order makes it very difficult to accurately predict their superstructures. Nonetheless, we can attempt to understand structural motifs based on the possible macrocyclic constructs (see Figure S1 in the Supporting Information). On the basis of the most stable bonding angles, there are two most plausible configurations for macrocycles: hexagon and pentagon. In an ordered Box-COP, e.g., COP-93, that is formed from simple hexagons, the pore opening should have been 20 Å, based on minimizations from both Materials Studio and Avogadro software that use universal force fields (see Figure 1d and Figure S1 in the Supporting Information). If pentagons are formed (similar to the statistical possibility in bucky balls) the pores have the widest opening of 15 Å. The experimental pore size distribution of COP-93 is 4.36 Å (Figure 2), indicating a

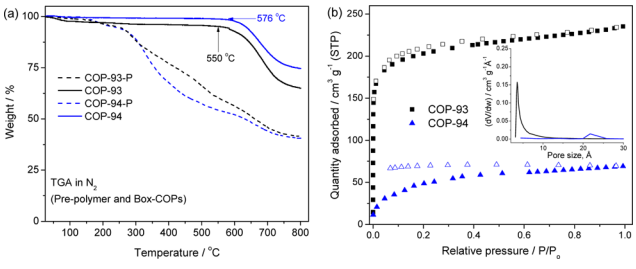

Figure 2. Thermal stability and porosity of Box-COPs. (a) Mass loss characteristics with temperature for prepolymers and thermal stability of Box-COPs, (b) Ar adsorption−desorption isotherms. Inset: NLDFT pore size distribution.

further penetration since we believe that even hexagons are randomly oriented (spirals, helixes). In an ideal ordered structure, we ought to see a major peak of pore widths similar to the basic hexagon. Hexagons are interpenetrated, even twice on the same macrocycle (Figure 1d) due to lack of large pores within polymeric network which results pore sizes below 5 Å. In reality, we believe that possible formation of both interpenetrated networks and/or solid-state packing of the polymeric networks could contribute to the observed narrow pore size of COP-93.

RESULTS AND DISCUSSION

The structures of silylated monomers, pre−polymers and Box-COPs were analyzed by FT−IR, ^{1}H NMR, CP/MAS ^{13}C NMR, and elemental analysis. ^{1}H NMR show chemical shifts at 6.24−6.27 ppm (Ar−H), 3.65 ppm (N−H), 1.00−0.97 ppm ($(CH_3)_3$), 0.24−0.2 ppm ($Si(CH_3)_2$), confirming the silylation of the monomers, which is also supported by FT−IR frequency at 3397 cm^{-1} (N−H), 2953 cm^{-1} (Ar−H), and 2862 cm^{-1} (CH_3).[46] Pre−polymers reveal characteristic IR peaks of the amide bonding, 1658 cm^{-1} (C═O) and 1526 (N−H) cm^{-1}, which clearly indicates the formation of prepolymers (see Figure S2a in the Supporting Information). A peak at 1366 cm^{-1} (CH_3) also suggesting that the hydroxyl group is protected by silylated functionality which provide excellent solubility of prepolymers in NMP. Pre−polymers were also characterized by solid-state CP/MAS ^{13}C NMR (see Figure S3a in the Supporting Information), which show chemical shifts at around 171.6 (C═O), 153.4 (Ph−O), 127.8 (Ph−NH), and 32.3−2.8 ppm ($Si(CH_3)_2C(CH_3)_3$). The benzoxazole ring formation after annealing prepolymers at 400 °C for 3 h is confirmed from the characteristic peaks at around 1618 cm^{-1} (C═N) and 1425, 1054 cm^{-1} (benzoxazole ring) (see Figure S2b in the Supporting Information). Indeed, CP/MAS ^{13}C NMR spectrum (see Figure S3b in the Supporting Information) of Box-COPs show chemical shifts that are assigned for each spectrum with respective structure. 168.4, 155.2, and 145.9 (benzoxazole ring), 134.7 and 118.1 ppm (Ph), supporting the formation of the benzoxazole linkages.[47] The experimental elemental analysis of Box-COPs is also in accordance with the theoretical values (see Table S1 in the Supporting Information). The cyclization of benzoxazole ring in Box-COPs from prepolymers was also monitored through TGA in N_2 environment (Figure 2a). The mass loss observed for prepolymers in the range of 150−500 °C was attributed to the deprotection of hydroxyl functionality, i.e. ,removal of silyl moiety and subsequent benzoxazole ring formation by dehydration. TGA study revealed that Box-COPs show unprecedented high thermal stability and almost no mass loss up to 550 and 576 °C for COP-93 and COP-94, respectively, under a N_2 atmosphere. In an oxidative environment, COP-93 and COP-94 are stable up to 378 and 450 °C, respectively (see Figure S4 in the Supporting Information).

The porous properties of Box-COPs were evaluated from the Ar adsorption−desorption isotherms measured at 87 K (Figure 2b), showing typical type I reversible isotherms. The isotherms displayed rapid Ar uptake at the very low relative pressure (<0.01), indicative of the characteristics of the permanent micropores. The specific surface area was determined by the Brunauer−Emmett−Teller (BET) method at relative pressure between 0.01−0.25 (see Figure S5 in the Supporting Information). The BET surface areas of COP-93 and COP-94 were found to be 606 and 80 m^2 g^{-1}, respectively (Table 1).

dx.doi.org/10.1021/cm503627p | *Chem. Mater.* 2014, 26, 6729−6733

Table 1. Surface Area, Pore Size, CO_2 Capture Capacity, CO_2/N_2 Selectivity, and Isosteric Heat of Adsorption of Box-COPs

				CO_2 adsorption at 1 bar (mg g^{-1})			CO_2/N_2 selectivity[d]			
Box-COPs	BET_{Ar}[a] (m^2 g^{-1})	BET_{CO_2}[b] (m^2 g^{-1})	pore size[c] (Å)	273 K	298 K	323 K	273 K	298 K	323 K	Q_{st}[e] (kJ mol^{-1})
COP-93	606	336	4.36	139.6	91.1	60.7	65.3	36.4	35.4	25.6
COP-94	80	229	20.3	94.1	59.1	40.5	49.8	33.9	48.0	26.2

[a]BET from Ar adsorption isotherms. [b]BET from CO_2 adsorption isotherms 273 K, [c]Median pore size from NLDFT. [d]CO_2/N_2 selectivity was measured by IAST method for CO_2:N_2 gas mixture of 15:85. [e]Isosteric heat of adsorption (Q_{st}) at initial loading.

The formation of interpenetrated polymeric network could be the reason behind the low surface area for COP-94, where the linker has a mandatory tilting because of its biphenylic construct. An open hysteresis loop is formed by the irreversible adsorption and desorption branches for COP-94, which is attributed to pore network effects. The BET surface areas were also measured from CO_2 isotherms at 273 K, demonstrating specific surface areas of 336 and 229 m^2 g^{-1} for COP-93 and COP-94, respectively. The Langmuir surface areas of COP-93 and COP-94 are 960 and 311 m^2 g^{-1}, respectively. Nonlocal density functional theory (NLDFT) pore size distributions using a slit pore model indicate a significant fraction of the pores surface originates from micropores with the average pore sizes of 4.36 and 20.3 Å for COP-93 and COP-94, respectively. The total pore volume, estimated from the amount adsorbed at relative pressure = 0.95, is 0.28 and 0.08 cm^3 g^{-1} for COP-93 and COP-94. Although the microporosity in Box-COPs are permanent and demonstrated similar surface area for repeated synthesis, the polymeric network lacks ordered structure as depicted in the XRD patterns (see Figure S6 in the Supporting Information), indicating formation of amorphous polymers.

We investigated the CO_2 and N_2 sorption isotherms of Box-COPs at 273, 298, and 323 K (Figure 3). CO_2 sorption isotherms show CO_2 uptake is rapid in the initial stage, implying that CO_2 molecule has favorable interaction with the Box-COPs network. The reversibility of adsorption−desorption curves with almost no hysteresis suggest feasibility of these structures for the practical application in CO_2 capture and regeneration. CO_2 capture capacity of COP-93 and COP-94 at 1 bar is 139.6 and 94.1 mg g^{-1} at 273 K, 91.1 and 59.1 mg g^{-1} at 298 K, and 60.7 and 40.5 mg g^{-1} at 323 K, respectively. It should be noted that the CO_2 capacity of COP-93 persistently increases with a rise in the pressure, and has not reached saturation at 1 bar, indicating that higher CO_2 sorption capacity can be achieved at even higher pressures. The high CO_2 uptakes are mainly attributed to the nanoporous nitrogen- and oxygen-rich polymeric network of COPs. It has been reported that the electron-rich networks can yield strong dipole−quadrupole interaction with CO_2, leading to a significant increase in the CO_2 adsorption capacity.[48] The leading CO_2 adsorbents, especially nanoporous polymeric networks with nitrogen and/or oxygen-rich frameworks, include CPOP-1 (212 mg g^{-1}),[28] PPF-1 (267 mg g^{-1}),[43] BILP-4 (235 mg g^{-1}),[48] ALP-1 (236 mg g^{-1}),[49] PPN-6-CH2DETA (189 mg g^{-1}),[50] and TB-COP-1 (228 mg g^{-1}).[51]

High selectivity of CO_2 over N_2 is one of the necessary characteristics for an adsorbent to be used for CO_2 capture. CO_2 and N_2 isotherms were fitted by Langmuir−Freundlich dual sites or Langmuir single site models to obtain CO_2/N_2 selectivity through ideal adsorbed solution theory (IAST) for the mixture of CO_2 and N_2 gas in the ratio of 15:85 (see Figure S7 in the Supporting Information). Researchers have been predicting and calculating IAST selectivity through various

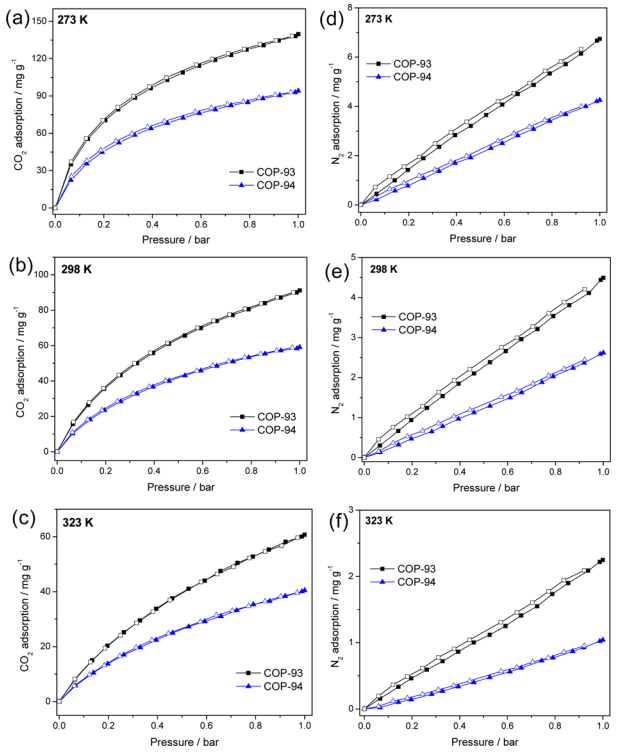

Figure 3. CO_2 adsorption−desorption isotherms for Box-COPs at (a) 273, (b) 298, and (c) 323 K. N_2 adsorption−desorption isotherms at (d) 273, (e) 298, and (f) 323 K.

models. İslamoğlu et al.[52] compared CO_2/N_2 selectivities obtained from three methods and showed that values depend on the method used. Here, we calculated CO_2/N_2 selectivities of Box-COPs by considering partial pressures of CO_2 and N_2 in a flue gas mixture as well as competition between gas molecules for binding sites.[52] The CO_2/N_2 selectivity of COP-93 and COP-94 at 1 bar is 65.3 and 49.8 at 273 K, 36.4 and 33.9 at 298 K, and 35.4 and 48 at 323 K, respectively. The CO_2/N_2 selectivity decreased at 298 K; however, it enhanced at 323 K. The reason behind this behavior is that the CO_2 binding affinity toward electron-rich network did not deteriorate as much as for N_2 binding. CO_2/N_2 selectivity is also substantially decreased with the rise in pressure, mainly because of a pressure-driven pore-filling mechanism irrespective of CO_2-philic sites (Figure 4). CO_2/N_2 selectivity values are comparable to other porous polymer networks and carbonaceous materials (see Table S2 in the Supporting Information).[43,48,52,53]

The isosteric heat (Q_{st}) of CO_2 adsorption is a central parameter that dictates the affinity of the porous sorbent toward CO_2, which in turn plays a major role in determining the adsorption selectivity and the necessary energy to release the CO_2 during the regeneration step. Q_{st} of CO_2 adsorption

dx.doi.org/10.1021/cm503627p | Chem. Mater. 2014, 26, 6729−6733

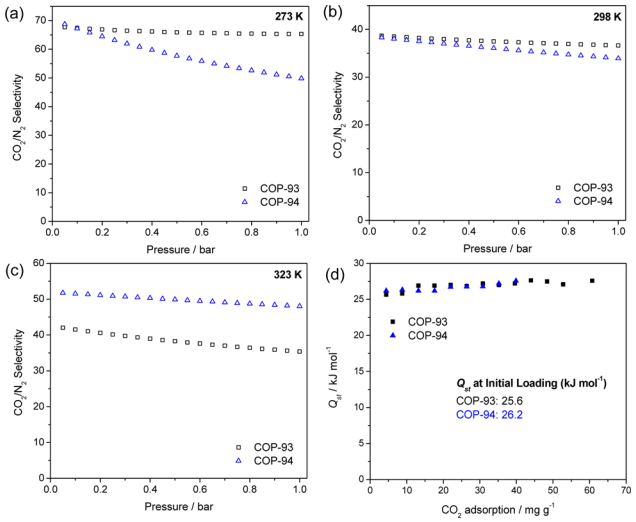

Figure 4. IAST CO_2/N_2 selectivities for CO_2:N_2 gas mixture (15:85) at (a) 273, (b) 298, and (c) 323 K. (d) Isosteric heat of CO_2 adsorption for Box-COPs.

for Box-COPs is around 25.6−26.2 kJ mol^{-1} at initial loading (Figure 4d), indicating CO_2 adsorption−desorption cycles can be achievable through pressure/vacuum swing sorption techniques. We studied the effect of boiling water on the stability of Box-COPs to mimic the harsh conditions sorbent may endure, since the exhaust gas contains water vapor and the water stability of CO_2 sorbents is one of the key requirements for practical CCS applications. The CO_2 capture capacities of Box-COPs after this treatment was also measured. Interestingly, Box-COPs showed no loss in CO_2 uptake efficiency after being boiled for a week, suggesting their robust nature (see Figure S8 in the Supporting Information). For the effect of moisture in CO_2 uptake (as industrial flue gases always contain), we anticipate that the capacities will certainly differ in humid conditions, although it may or may not be as significant.

CONCLUSIONS

In summary, we reported the first set of processable, electron-rich, and highly thermally stable Box-COPs with permanent microporosity. Silylation of building blocks facilitate control over network formation and processability, pointing the method's potential in other heterocyclic porous networks, such as imidazoles, oxadiazoles, triazoles, tetrazines. The synthesis also benefits from not needing to use rare earth catalysts, a significant issue when scale up is considered. An excellent CO_2 capture capacity (139.6 mg g^{-1} at 273 K and 1 bar) with low Q_{st} (25.6−26.2 kJ mol^{-1}) was achieved in an amorphous nanoporous polymeric network. Box-COPs showed unprecedented thermal stability up to 576 °C and CO_2 capture capacity did not hinder after boiling in water for a week. Because of facile adsorption−desorption characteristics, these sorbents provide effective regeneration capability without the use of addition energy and also show moderate CO_2/N_2 selectivities at elevated temperatures. Using our strategies presented here, a series of benzoxazole polymeric networks can easily be synthesized for physisorption- or membrane-based CO_2 capture technologies.

EXPERIMENTAL SECTION

Synthesis of Box-COPs (see detailed procedure in the Supporting Information). The silylated monomers were synthesized by reaction of *tert*-butyldimethylsilyl chloride with 4,6-diaminoresorcinol dihydrochloride and 3,3′-dihydroxybenzidine in *N*,*N*-dimethylformamide in the presence of triethylamine at 25 °C for 24 h. The silylated monomers were then thoroughly washed with water and dried at 80 °C under a vacuum overnight. These functionalized monomers reacted with 1,3,5-benzenetricarbonyl trichloride in *N*-methyl-2-pyrrolidone (NMP) at 5−25 °C for 24 h, which results in prepolymers. The prepolymers were separated from NMP by evaporating 80% of solvents under vacuum in rotary evaporator and remaining mixture was added to water, which produced precipitates. These precipitates were washed with water and dried. The prepolymers were heated to 400 °C at 2 °C min^{-1} under vacuum for 3 h to obtain Box-COPs.

Structural Characterization and Gas Sorption. Solid-state cross-polarization magic angle spinning (CP/MAS) ^{13}C NMR spectra collected by a Bruker Avence III 400 WB NMR spectrometer. FT−IR spectra were recorded on KBr pellets. Ar adsorption−desorption isotherms were obtained with a Micromeritics 3Flex accelerated surface area and porosimetry analyzer at 87 K, after the samples had been degassed at 150 °C for 5 h under vacuum. CO_2 and N_2 adsorption−desorption isotherms for Box-COPs were measured at 273, 298, and 323 K using a static volumetric system. The temperature during adsorption and desorption was kept constant using a temperature controller. Prior to the adsorption measurements, the samples were dried at 150 °C for 5 h. All the adsorption−desorption experiments were carried out twice to ensure the reproducibility. There were no noticeable differences in the isotherm points obtained from both experiments.

ASSOCIATED CONTENT

Supporting Information

Synthesis, FT−IR, CP/MAS ^{13}C NMR, elemental analysis, TGA. IAST fitting curves, Q_{st}, and boiling water stability. This material is available free of charge via the Internet at http://pubs.acs.org.

AUTHOR INFORMATION

Corresponding Author

*E-mail: yavuz@kaist.ac.kr. Fax: +82 42 350 2248. Tel: +81 42 350 1718.

Notes

The authors declare no competing financial interest.

ACKNOWLEDGMENTS

We acknowledge the financial support by grants from Korea CCS R&D Centre, Basic Science Research Program (2013R1A1A1012998), and IWT (NRF-2012-C1AAA001-M1A2A2026588), funded by National Research Foundation of Korea (NRF) under the Ministry of Science, ICT & Future Planning of Korean government.

REFERENCES

(1) Chen, I. C.; Hill, J. K.; Ohlemuller, R.; Roy, D. B.; Thomas, C. D. *Science* **2011**, *333*, 1024−1026.
(2) D'Alessandro, D. M.; Smit, B.; Long, J. R. *Angew. Chem., Int. Ed.* **2010**, *49*, 6058−6082.
(3) Mora, C.; Frazier, A. G.; Longman, R. J.; Dacks, R. S.; Walton, M. M.; Tong, E. J.; Sanchez, J. J.; Kaiser, L. R.; Stender, Y. O.; Anderson, J. M.; Ambrosino, C. M.; Fernandez-Silva, I.; Giuseffi, L. M.; Giambelluca, T. W. *Nature* **2013**, *502*, 183−187.
(4) Monastersky, R. *Nature* **2013**, *497*, 13−14.
(5) Bae, T. H.; Hudson, M. R.; Mason, J. A.; Queen, W. L.; Dutton, J. J.; Sumida, K.; Micklash, K. J.; Kaye, S. S.; Brown, C. M.; Long, J. R. *Energy Environ. Sci.* **2013**, *6*, 128−138.
(6) Goeppert, A.; Czaun, M.; May, R. B.; Prakash, G. K. S.; Olah, G. A.; Narayanan, S. R. *J. Am. Chem. Soc.* **2011**, *133*, 20164−20167.

(7) Sevilla, M.; Fuertes, A. B. *Energy Environ. Sci.* **2011**, *4*, 1765−1771.
(8) Srinivas, G.; Krungleviciute, V.; Guo, Z. X.; Yildirim, T. *Energy Environ. Sci.* **2014**, *7*, 335−342.
(9) Sumida, K.; Rogow, D. L.; Mason, J. A.; McDonald, T. M.; Bloch, E. D.; Herm, Z. R.; Bae, T. H.; Long, J. R. *Chem. Rev.* **2012**, *112*, 724−781.
(10) Zhou, H. C.; Long, J. R.; Yaghi, O. M. *Chem. Rev.* **2012**, *112*, 673−674.
(11) Aron, D.; Tsouris, C. *Sep. Sci. Technol.* **2005**, *40*, 321−348.
(12) Du, N. Y.; Park, H. B.; Robertson, G. P.; Dal-Cin, M. M.; Visser, T.; Scoles, L.; Guiver, M. D. *Nat. Mater.* **2011**, *10*, 372−375.
(13) McKeown, N. B.; Budd, P. M. *Macromolecules* **2010**, *43*, 5163−5176.
(14) Park, H. B.; Jung, C. H.; Lee, Y. M.; Hill, A. J.; Pas, S. J.; Mudie, S. T.; Van Wagner, E.; Freeman, B. D.; Cookson, D. J. *Science* **2007**, *318*, 254−258.
(15) Patel, H. A.; Yavuz, C. T. *Chem. Commun.* **2012**, *48*, 9989−9991.
(16) Patel, H. A.; Je, S. H.; Park, J.; Chen, D. P.; Jung, Y.; Yavuz, C. T.; Coskun, A. *Nat. Commun.* **2013**, *4*, 1372.
(17) Wan, S.; Gandara, F.; Asano, A.; Furukawa, H.; Saeki, A.; Dey, S. K.; Liao, L.; Ambrogio, M. W.; Botros, Y. Y.; Duan, X. F.; Seki, S.; Stoddart, J. F.; Yaghi, O. M. *Chem. Mater.* **2011**, *23*, 4094−4097.
(18) Gopalakrishnan, D.; Dichtel, W. R. *J. Am. Chem. Soc.* **2013**, *135*, 8357−8362.
(19) Totten, R. K.; Kim, Y. S.; Weston, M. H.; Farha, O. K.; Hupp, J. T.; Nguyen, S. T. *J. Am. Chem. Soc.* **2013**, *135*, 11720−11723.
(20) Ben, T.; Ren, H.; Ma, S. Q.; Cao, D. P.; Lan, J. H.; Jing, X. F.; Wang, W. C.; Xu, J.; Deng, F.; Simmons, J. M.; Qiu, S. L.; Zhu, G. S. *Angew. Chem., Int. Ed.* **2009**, *48*, 9457−9460.
(21) Dawson, R.; Cooper, A. I.; Adams, D. J. *Prog. Polym. Sci.* **2012**, *37*, 530−563.
(22) Thomas, A. *Angew. Chem., Int. Ed.* **2010**, *49*, 8328−8344.
(23) Feng, X.; Ding, X. S.; Jiang, D. L. *Chem. Soc. Rev.* **2012**, *41*, 6010−6022.
(24) Jing, X. F.; Zou, D. L.; Cui, P.; Ren, H.; Zhu, G. S. *J. Mater. Chem. A* **2013**, *1*, 13926−13931.
(25) Xu, Y. H.; Jin, S. B.; Xu, H.; Nagai, A.; Jiang, D. L. *Chem. Soc. Rev.* **2013**, *42*, 8012−8031.
(26) Biswal, B. P.; Chandra, S.; Kandambeth, S.; Lukose, B.; Heine, T.; Banerjee, R. *J. Am. Chem. Soc.* **2013**, *135*, 5328−5331.
(27) Carta, M.; Malpass-Evans, R.; Croad, M.; Rogan, Y.; Jansen, J. C.; Bernardo, P.; Bazzarelli, F.; McKeown, N. B. *Science* **2013**, *339*, 303−307.
(28) Chen, Q.; Luo, M.; Hammershoj, P.; Zhou, D.; Han, Y.; Laursen, B. W.; Yan, C. G.; Han, B. H. *J. Am. Chem. Soc.* **2012**, *134*, 6084−6087.
(29) Colson, J. W.; Dichtel, W. R. *Nat. Chem.* **2013**, *5*, 453−465.
(30) El-Kaderi, H. M.; Hunt, J. R.; Mendoza-Cortes, J. L.; Cote, A. P.; Taylor, R. E.; O'Keeffe, M.; Yaghi, O. M. *Science* **2007**, *316*, 268−272.
(31) Farha, O. K.; Bae, Y. S.; Hauser, B. G.; Spokoyny, A. M.; Snurr, R. Q.; Mirkin, C. A.; Hupp, J. T. *Chem. Commun.* **2010**, *46*, 1056−1058.
(32) Jiang, J. X.; Su, F.; Trewin, A.; Wood, C. D.; Campbell, N. L.; Niu, H.; Dickinson, C.; Ganin, A. Y.; Rosseinsky, M. J.; Khimyak, Y. Z.; Cooper, A. I. *Angew. Chem., Int. Ed.* **2007**, *46*, 8574−8578.
(33) Martin, C. F.; Stockel, E.; Clowes, R.; Adams, D. J.; Cooper, A. I.; Pis, J. J.; Rubiera, F.; Pevida, C. *J. Mater. Chem.* **2011**, *21*, 5475−5483.
(34) Patel, H. A.; Karadas, F.; Byun, J.; Park, J.; Deniz, E.; Canlier, A.; Jung, Y.; Atilhan, M.; Yavuz, C. T. *Adv. Funct. Mater.* **2013**, *23*, 2270−2276.
(35) Patel, H. A.; Karadas, F.; Canlier, A.; Park, J.; Deniz, E.; Jung, Y.; Atilhan, M.; Yavuz, C. T. *J. Mater. Chem.* **2012**, *22*, 8431−8437.
(36) Rabbani, M. G.; El-Kaderi, H. M. *Chem. Mater.* **2011**, *23*, 1650−1653.
(37) Schwab, M. G.; Fassbender, B.; Spiess, H. W.; Thomas, A.; Feng, X.; Mullen, L. K. *J. Am. Chem. Soc.* **2009**, *131*, 7216−7217.
(38) Xie, L. H.; Suh, M. P. *Chem. Eur. J.* **2013**, *19*, 11590−11597.
(39) Xie, Z. G.; Wang, C.; deKrafft, K. E.; Lin, W. B. *J. Am. Chem. Soc.* **2011**, *133*, 2056−2059.
(40) Yuan, D. Q.; Lu, W. G.; Zhao, D.; Zhou, H. C. *Adv. Mater.* **2011**, *23*, 3723−3725.
(41) Zhang, D. S.; Chang, Z.; Lv, Y. B.; Hu, T. L.; Bu, X. H. *RSC Adv.* **2012**, *2*, 408−410.
(42) Zhu, X.; Do-Thanh, C. L.; Murdock, C. R.; Nelson, K. M.; Tian, C. C.; Brown, S.; Mahurin, S. M.; Jenkins, D. M.; Hu, J.; Zhao, B.; Liu, H. L.; Dai, S. *ACS Macro Lett.* **2013**, *2*, 660−663.
(43) Zhu, Y. L.; Long, H.; Zhang, W. *Chem. Mater.* **2013**, *25*, 1630−1635.
(44) So, Y. H.; Heeschen, J. P. *J. Org. Chem.* **1997**, *62*, 3552−3561.
(45) Fukumaru, T.; Fujigaya, T.; Nakashima, N. *Macromolecules* **2012**, *45*, 4247−4253.
(46) Fukumaru, T.; Fujigaya, T.; Nakashima, N. *Polym. Chem.* **2012**, *3*, 369−376.
(47) Tullos, G. L.; Powers, J. M.; Jeskey, S. J.; Mathias, L. J. *Macromolecules* **1999**, *32*, 3598−3612.
(48) Rabbani, M. G.; El-Kaderi, H. M. *Chem. Mater.* **2012**, *24*, 1511−1517.
(49) Arab, P.; Rabbani, M. G.; Sekizkardes, A. K.; İslamoğlu, T.; El-Kaderi, H. M. *Chem. Mater.* **2014**, *26*, 1385−1392.
(50) Lu, W.; Sculley, J. P.; Yuan, D.; Krishna, R.; Wei, Z.; Zhou, H. C. *Angew. Chem., Int. Ed.* **2012**, *51*, 1−6.
(51) Byun, J.; Je, S. H.; Patel, H. A.; Coskun, A.; Yavuz, C. T. *J. Mater. Chem. A.* **2014**, *2*, 12507−12512.
(52) İslamoğlu, T.; Rabbani, M. G.; El-Kaderi, H. M. *J. Mater. Chem. A.* **2013**, *2*, 10559−10266.
(53) Patel, H. A.; Je, S. H.; Park, J.; Jung, Y.; Coskun, A.; Yavuz, C. T. *Chem.—Eur. J.* **2013**, *20*, 772−780.